

# Documentation of the chromatic aberration correction plug-in for ImageJ

Julien PONTABRY

September 21, 2015

## Abstract

Despite modern microscopes are diffraction limited, chromatic aberrations remains a critical issue for image analysis of small structures. The chromatic aberration correction plug-in for ImageJ is designed to remove such artefact and this document aims to be a guide for users.

## Contents

<b>1</b>	<b>Introduction</b>	<b>2</b>
<b>2</b>	<b>Chromatic shift estimation with micro-beads</b>	<b>2</b>
<b>3</b>	<b>Dense chromatic field reconstruction</b>	<b>3</b>
<b>4</b>	<b>Graphical user interface</b>	<b>4</b>
<b>5</b>	<b>Implementation details</b>	<b>5</b>
<b>6</b>	<b>Use case</b>	<b>6</b>
<b>7</b>	<b>References</b>	<b>7</b>

# 1 Introduction

Modern confocal microscopes are diffraction limited, i.e. the chromatic shift is expected to be less than  $0.2\ \mu\text{m}$  on the lateral view and less than  $0.5\ \mu\text{m}$  on the axial view (Manders 1997). Although for large structure the chromatic shift is negligible, image quantification of small structures may be very sensitive to chromatic aberrations and therefore may require a correction.

The most efficient way to correct for chromatic shift is to calibrate the microscope with images of micro-beads (called calibration images). These images, acquired simultaneously with input images and with the same settings, are used to evaluate the chromatic field. Because the shape of the micro-beads is known a priori, the chromatic shift between different wavelength can be accurately estimated.

The chromatic shift correction plug-in implements a two-step strategy: i) the sparse chromatic field is estimated by detection of micro-beads in calibration images (Kozubek et al. 2000) and ii) the chromatic field over the whole image is interpolated with the bi-harmonic spline method (Sandwell 1987). This document is meant to describe the use the ImageJ plug-in for chromatic aberration correction.

The rest of this document is subdivided into five sections. First, the two steps of the correction algorithm are explained. Then the graphical user interface and implementation details are described. Finally, an example of use is given.

## 2 Chromatic shift estimation with micro-beads

The first step of the algorithm, i.e. detecting the micro-beads in both channels of each calibration image and produce a sparse chromatic field, is performed following the method described by Kozubek et al. (2000).

First a rough segmentation of micro-beads is performed on the first channel with Yen’s thresholding method (Sezgin et al. 2004). Then the segmented objects are filtered by their size, in order to keep only alone beads. The centres of resulting objects are used to define a region of interest (ROI) of 21 pixels side<sup>1</sup> around the beads. Again, to avoid bad shift estimation, the ROI are filtered such that only non-overlapping and non-touching ROI are kept.

Then, for both channels and for each ROI, the centre of the bead can be estimated accurately with an intensity-weighted sum:

$$C_k = \frac{\sum_{p \in \mathcal{V}} p_k I(p)}{\sum_{p \in \mathcal{V}} I(p)}, \quad (1)$$

where  $p$  denotes the coordinates of a voxel,  $I(p)$  is the intensity of voxel  $p$ ,  $k$  denotes the component (either  $x$ ,  $y$  or  $z$ ) and  $\mathcal{V}$  is the set of pixel inside the current ROI with intensity  $I(p) \geq 0.5 \times (I_{min} + I_{max})$  ( $I_{min}$  and  $I_{max}$  are respectively the min and max intensity inside ROI).

Finally, for each ROI, the vector corresponding to the chromatic shift is defined by the centres of both channels. By accumulating all ROI and all calibration images, a sparse chromatic field is created (see figure 1).

### 3 Dense chromatic field reconstruction

A sparse field as estimated in section 2 is not enough to correct the entire image domain, unless a very large number of calibration images are acquired. Hopefully, the sparse field usually contains enough information to estimate a dense field by interpolation. In the plug-in, the bi-harmonic spline interpolation method has been implemented. This technique has first be used for satellite data interpolation (Sandwell 1987).

---

<sup>1</sup>here we assume that the shift is well below 21 pixels

When Green's functions are used to interpolate  $N$  data points  $f_i$  located at  $p_i$  in dimension  $M$  to produce an interpolated function  $f$ , the problem to solve is described by the following equation:

$$\nabla^4 f(p) = \sum_{j=1}^N \omega_j \delta(p - p_j) \text{ with } f(p_i) = f_i \text{ ,} \quad (2)$$

where  $\nabla^4$  is the bi-harmonic operator. The general solution to this problem is given by

$$f(p) = \sum_{j=1}^N \omega_j \Phi_M(p - p_j) \text{ ,} \quad (3)$$

where  $\Phi_M$  is the  $M$ -dimensional Green's function. The weights  $\omega_j$  are found by solving the following linear system:

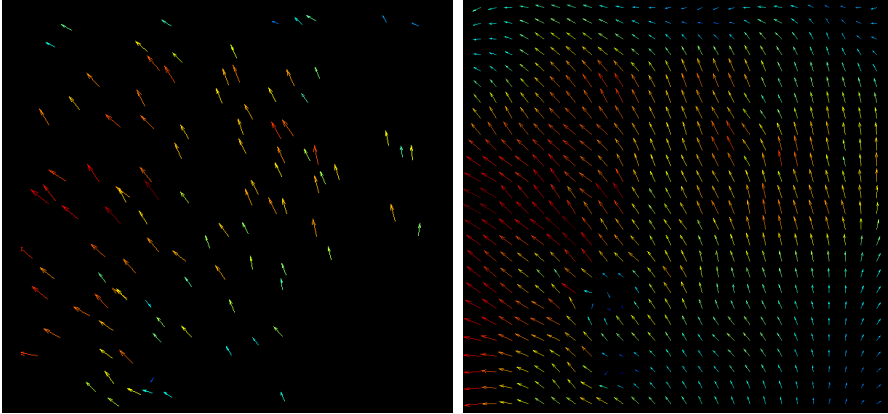
$$f_i = \sum_{j=1}^N \omega_j \Phi_M(p_i - p_j) \text{ .} \quad (4)$$

Once the weights  $\omega_j$  are estimated, the function (3) is used to evaluate the chromatic field at each point in the image domain. An example of field interpolation is depicted in figure 1.

## 4 Graphical user interface

Once installed, the plug-in can be found in menu Plugins > Restoration > Chromatic shift correction with beads. As shown in figure 2, the graphical user interface (GUI) of the plug-in asks for a few inputs/outputs and two parameters that are detailed below:

- the *Calibration(s)* text area is used to set a path to a folder of micro-beads images or to a file, either a micro-beads image or a pre-computed chromatic field;
- the *Input image(s)* text area is used to set a path to input image(s), either a folder or a file;



(a) Sparse field

(b) Interpolated field

Figure 1: Example of chromatic field interpolation. Left: the sparse chromatic field after beads detection; right: the same field after bi-harmonic spline interpolation over the whole image domain. Colours indicate magnitudes of vectors (from blue, low magnitude to red, high magnitude).

- the *Output chromatic field* text area is used to set a path of a file, in which the chromatic field computed with micro-beads will be written;
- the *Output image(s)* text area is used to set a path to a folder where the corrected input image(s) will be written;
- the *Channel to be corrected* option is used to decide which channel will be shifted with the chromatic field;
- the *Bead's diameter* parameter is used to set the diameter of the micro-beads in calibration image(s).

## 5 Implementation details

The weights of the interpolation function in section 3 are found by solving a system of linear equations as (4), for  $i = 0, \dots, N$ . This

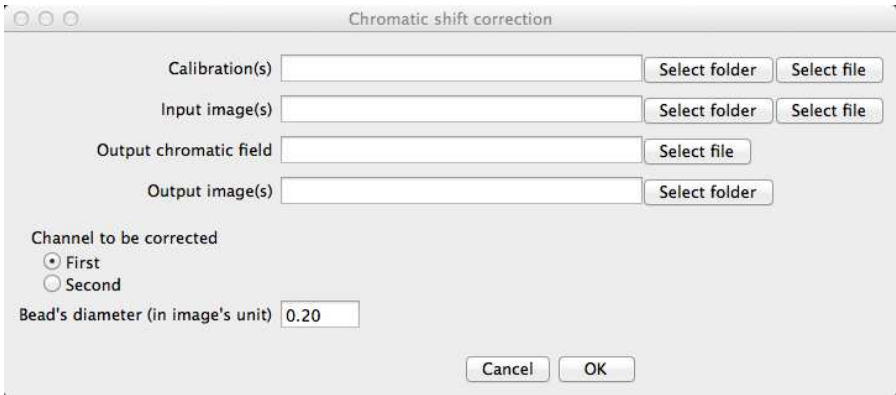


Figure 2: Graphical user interface (GUI) of the plug-in.

system can be written with matrices:

$$G\omega = f , \quad (5)$$

where  $\omega$  is the vector of weights,  $f$  is the vector of response and  $G$  is the matrix of Green's function. This linear system is solved by inverting the matrix  $G$ :

$$\omega = G^{-1}f . \quad (6)$$

To invert  $G$ , the Gauss-Jordan reduction algorithm has been implemented in the plug-in. The principle is to modify the matrix such that the inverse can be computed easily. First, the matrix is arranged to make it superior triangular and then, the inverse is computed. Permutation of lines and columns has been implemented, in order to improve robustness to rounding errors during the reduction.

## 6 Use case

For this use case, we would like to study a small zebra structures of *C. elegans* (see figure 4). The filament structure has an approximate size of  $0.1\mu\text{m}$  (about 1 pixel on image). Two markers with

different emission wavelength have been used: 491 nm and 561 nm. Note that despite the wavelengths are close, the measured chromatic shift is about 1 pixel, which is the size of the structure under study. Here the question is to know if the filament structures are co-localising or interleaved.

In addition with the acquisition of sample images, three calibration images have been acquired with exactly the same set-up (see figure 3). The radius of the beads is about 0.2  $\mu\text{m}$ .

The plug-in has been used to correct the chromatic shift with the following parameters: the first channel has been shifted and the bead's diameter has been set to 0.4  $\mu\text{m}$ . Close-up examples before and after corrections are shown for one calibration image and input image respectively in figures 3 and 4.

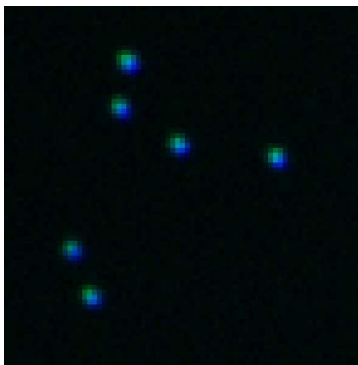
Without the chromatic shift correction, the analysis of the structures results in co-localising pattern: the Spearman's coefficient, equal to 0.16, is significantly different from 0 (considering 95% confidence bounds). With the correction, the analysis of the structures results in interleaved pattern: the Spearman's coefficient, equal to -0.18, is also significantly different from 0. The conclusions of both analysis are in opposition and both Spearman's coefficient are statistically significant. However, without chromatic shift correction, the results and the subsequent interpretation are incorrect.

## 7 References

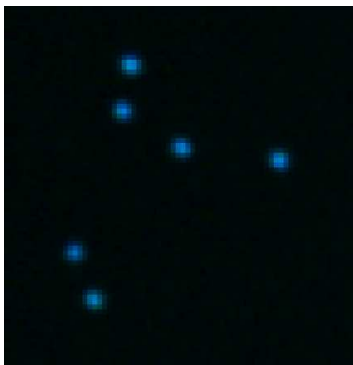
- Kozubek, M. and P. Matula (2000). "An efficient algorithm for measurement and correction of chromatic aberrations in fluorescence microscopy". In: *Journal of Microscopy* 200.3, pp. 206–217. ISSN: 1365-2818.
- Manders, E. M. M. (1997). "Chromatic shift in multicolour confocal microscopy". In: *Journal of Microscopy* 185.3, pp. 321–328. ISSN: 1365-2818.



(a) Calibration image

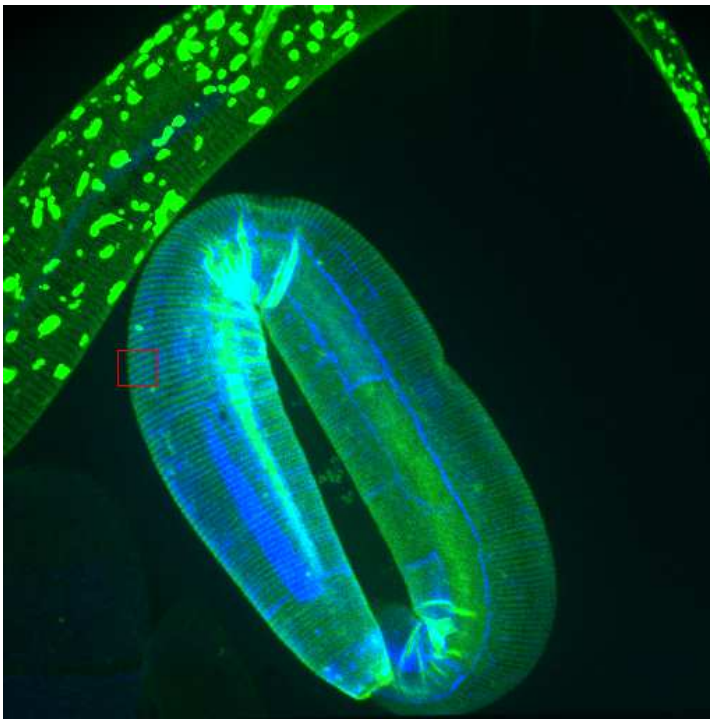


(b) Original - zoom

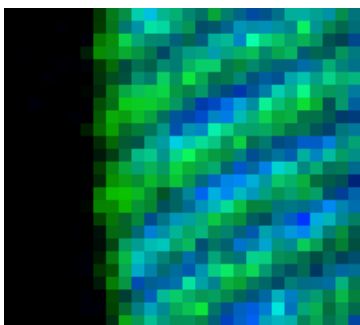


(c) Corrected - zoom

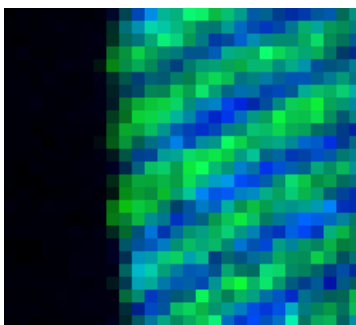
Figure 3: Correction example on a micro-bead image. The beads have a radius equal to  $0.2\ \mu\text{m}$ . The red square on top image depicts the zoom area.



(a) Input image



(b) Original - zoom



(c) Corrected - zoom

Figure 4: Correction example on a input image. The red square on top image depicts the zoom area.

- Sandwell, D.T. (1987). “Biharmonic Spline Interpolation of GEOS-3 and SEASAT Altimeter Data”. In: *Geophysical Research Letters* 14.2, pp. 139–142.
- Sezgin, M. and B. Sankur (2004). “Survey over image thresholding techniques and quantitative performance evaluation”. In: *Journal of Electronic Imaging* 13.1, pp. 146–165.